frontiers | Frontiers in Physics

TYPE Original Research
PUBLISHED 22 March 2023
DOI 10.3389/fphy.2023.1170895

OPEN ACCESS

EDITED BY
Baole Lu,
Northwest University, China

REVIEWED BY
Yudong Lian,
Hebei University of Technology, China
Quan Sheng,
Tianjin University, China
Bin Yin,
Ocean University of China, China

*CORRESPONDENCE
Fengping Yan,
fpyan@bjtu.edu.cn

SPECIALTY SECTION
This article was submitted to Optics and Photonics,
a section of the journal
Frontiers in Physics

RECEIVED 21 February 2023
ACCEPTED 13 March 2023
PUBLISHED 22 March 2023

CITATION
Guan B, Yan F, Qin Q, Liu Y, Yang D, Tan H, Li T, Yu C, Wang X, Jiang Y, Kumamoto K and Suo Y (2023), Thulium-doped fiber laser with switchable single-wavelength output using polarization-dependent loss.
Front. Phys. 11:1170895.
doi: 10.3389/fphy.2023.1170895

Thulium-doped fiber laser with switchable single-wavelength output using polarization-dependent loss

Biao Guan[1], Fengping Yan[1]*, Qi Qin[1], Yan Liu[1], Dandan Yang[1], Haoyu Tan[1], Ting Li[1], Chenhao Yu[1], Xiangdong Wang[1], Youchao Jiang[1], Kazuo Kumamoto[2] and Yuping Suo[3]

[1]School of Electronic and Information Engineering, Beijing Jiaotong University, Beijing, China, [2]Department of Electronics, Information and Communication Engineering, Osaka Institute of Technology, Osaka, Japan, [3]Department of Gynecology and Obstetrics, The Fifth Clinical Medical College of Shanxi Medical University, Taiyuan, China

A thulium-doped fiber laser (TDFL) with switchable single-wavelength output was proposed and experimentally constructed, and its output characteristics were investigated. The central wavelengths were 1940.52 nm and 2048.04 nm, defined by a superimposed uniform fiber Bragg grating (SI-UFBG) with reflectivity larger than 92%. Switchable output was successfully achieved by using polarization-dependent loss, with the help of a drop-in polarization controller and an in-line polarizer. For both output wavelengths, optical signal-to-noise ratios larger than 80 dB were achieved. Maximum fluctuations of the central wavelengths of 1940.52 nm and 2048.02 nm under 60 min were, respectively, 0.04 nm and 0.01 nm. Maximum fluctuations of output power for the same wavelengths over the same time period were, respectively, 1.09 dB and 0.12 dB. Maximum output powers of 215.12 mW and 155.53 mW were achieved for the respective output wavelengths of 1940.52 nm and 2048.02 nm. Moreover, a tuning range of ~2 nm was realized by enforcing a strain on the SI-UFBG. The proposed TDFL may be applied in laser medicine and free-space-related applications.

KEYWORDS

thulium-doped fiber laser, wavelength switchable output, superimposed fiber Bragg grating, tunable fiber laser, polarization-dependent loss

1 Introduction

The wide fluorescence spectrum of thulium-doped fiber (TDF) is up to 400 nm, and is located in an "eye-safe" wavelength region starting at 1,400 nm [1]. A low-loss atmospheric transmission window is also located in this waveband [2]. Thus, thulium-doped fiber lasers (TDFLs) have been widely investigated during the past few years, and have been used extensively in photoacoustic imaging [3], consolidation of thermoplastic coating [4], high-sensitivity strain sensors [5], dual-comb spectroscopy [6], generation of microwaves [7], laser surgery [8] and pump optical sources [9]. Researchers have also tried to obtain different output wavebands using TDFL, including 1.6 μm [10], 1.7 μm [11], 1.8 μm [12], 1.9 μm [13], 2.0 μm [14], and 2.05 μm wavebands [15].

Significantly, TDFL with an output central wavelength located in the 1.9 μm waveband, especially around 1940 nm, is found to be of vital importance in biomedicine. For example, Żywicka et al. compared the cutting efficiency and hemostasis effect of a TDFL working at

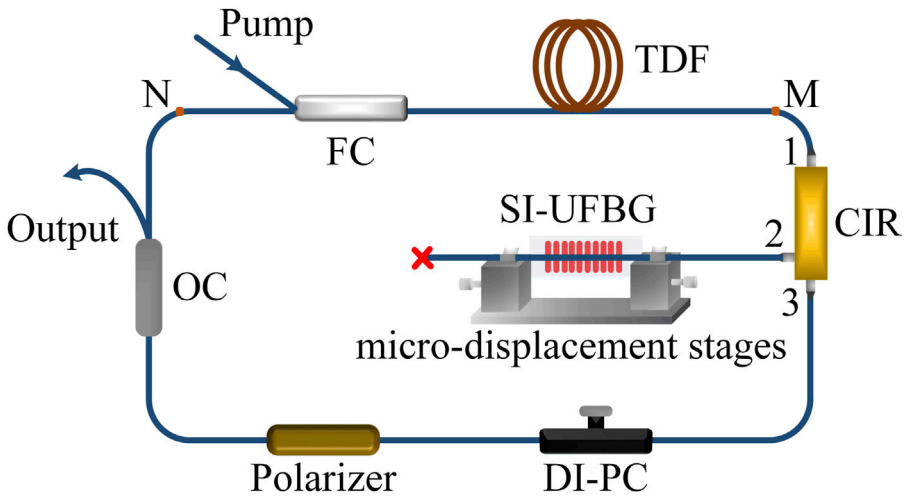

FIGURE 1
Schematic diagram of the TDFL. FC: fiber combiner; TDF: thulium-doped fiber; CIR: circulator; SI-UFBG: superimposed-uniform fiber Bragg grating; DI-PC: drop-in-polarization controller; OC: optical coupler.

1940 nm and a diode laser working at 1,470 nm. Their results demonstrated that TDFL produced a narrower zone of thermal damage [16]. TDFL was used as an energy device by Tendean et al. to reduce blood loss in liver parenchyma resection, and the retrospective study revealed that TDFL was a promising energy device in treating secondary liver tumors [17]. In addition, TDFL with an output central wavelength located in a longer waveband, such as ~2.05 μm, is important in free-space-related applications. For example, McComb et al. demonstrated that 2.05 μm IR radiation suffered less transmission loss than 1.94 μm radiation [18]. Thus, a free-space optical communication (FSOC) system operating at 2.05 μm is preferred. Our group has successfully demonstrated an FSOC system at 2.05 μm that is capable of real-time video transmission [19]. Noted that most previously reported TDFLs operated in the 1.94 μm or 2.05 μm waveband [20–24]. In 2022, our group proposed a TDFL with switchable output between 1941.312 nm and 2049.335 nm. However, the usage of two FBGs and a translation stage complicate the experimental configuration [25]. Thus, a compact high-performance TDFL with switchable output of 1.94 μm and 2.05 μm, capable of satisfying the above-mentioned applications simultaneously, is still worth investigating.

To realize switchable output in TDFLs, different wavelength switchable mechanisms have been proposed—for example, an in-line acousto-optic tunable bandpass filter [26], a digital micromirror array [27], a diffraction grating [28], polarization-dependent loss (PDL) [29], changing the temperature [30], applying strain [31], and enforcing axial misalignment [32]. It should be noted that digital micromirror arrays and diffraction gratings are expensive, making such TDFLs costly. Use of an in-line acousto-optic tunable bandpass filter and temperature control need additional active equipment, complicating the experimental configuration. To realize strain control and axial misalignment, micro-displacement equipment is usually incorporated, making the laser cavity bulky. However, PDL can be easily induced by inserting a polarization controller and an in-line polarizer that are compatible with the fiber structure of the laser cavity. In fact, however, using PDL to realize switchable output in TDFL has rarely been reported [33–35].

In this work, a TDFL with switchable single-wavelength output of ~1.94 μm and 2.05 μm is proposed and constructed. A superimposed fiber Bragg grating (SI-UFBG) was used to locate the lasing wavelength; the PDL was used to realize the switchable output. First, the experimental configuration was introduced, and the transmission and reflection characteristics of the SI-UFBG were measured. Then, the amplified spontaneous emission (ASE) spectra under forward and backward pumping schemes were investigated. Finally, the switchable output characteristics of the TDFL were described and the stability, power scaling, and tunability of the proposed TDFL were also studied in detail.

2 Materials and methods

2.1 Experimental setup

The configuration of the proposed TDFL is shown in Figure 1. Pump light of 793 nm was injected into the active media through a fiber combiner (FC, LightComm Technology Co.), and the pump fiber, signal fiber, and output fiber of the FC was respectively multimode fiber (SI 105/125-22/250, YOFC), single mode double-clad fiber (FUD-4070 SM-GDF-10/130-15FA, Nufern), and single mode double-clad fiber (FUD-4070 SM-GDF-10/130-15FA, Nufern). The maximum output power of the 793 nm pump source was 12 W, and the output power could be continuously adjusted manually. The active media was a spool of TDF (SM-TDF-10P/130M, Nufern.) with length of 1.73 m, and its core and cladding diameters were, respectively, 10 μm and 130 μm. The output of the TDF was connected with Port 1 of the circulator (CIR) and the transmission light was reflected by the SI-UFBG through Port 2 of the CIR. A drop-in polarization controller (DI-PC), followed by an in-line polarizer, was spliced with Port 3 of the CIR. The output of

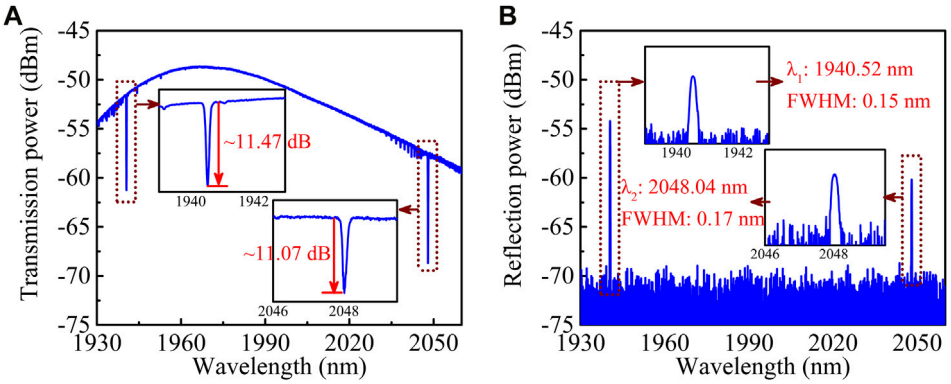

FIGURE 2
(A) Transmission and **(B)** reflection spectra of the SI-UFBG.

the in-line polarizer was spliced with the input of the optical coupler (OC), with a coupling ratio of 90:10, and the 90% output port was spliced with the signal port of the FC. The optical signal was monitored by a long-wavelength optical spectrum analyzer (OSA, AQ6375B, YOKOGAWA) from the 10% output port of the OC. The resolution and sampling rate of the OSA used in the experiment were 0.05 nm and 0.01 nm, respectively.

2.2 Measurement of the SI-UFBG

The SI-UFBG was fabricated by the phase mask method using a 248 nm excimer laser (ExciStar, Coherent) [36, 37]. Two phase masks with period of 1,347.3 nm and 1,423.7 nm were used to obtain two different channels located at ~1940 nm and 2050 nm, respectively. The fabrication process was as follows: First, a phase mask with a period of 1,347.3 nm was used to obtain the first Bragg wavelength of ~1940 nm. Then, a phase mask with a period of 1,423.7 nm was used to obtain the second Bragg wavelength of ~2050 nm, with other Bragg writing parameters unchanged. Thus, two Bragg wavelengths could be obtained easily.

A homemade thulium-doped fiber amplifier with an operating waveband of 1900 nm–2,100 nm was used as the wideband optical source to measure the transmission and reflection spectra of the SI-UFBG. The results are shown in Figures 2A, B. It can be seen in Figure 2A that two transmission dips are formed, which demonstrates the effectiveness of the exposure using two phase masks. The enlarged spectra around the two transmission dips are also shown in Figure 2A, and the respective transmission depth for ~1940 nm and ~2050 nm are ~11.47 dB and 11.07 dB, corresponding to reflectivities of 92.87% and 92.18%. The reflection spectrum with a wavelength span of 130 nm is shown in Figure 2B. Two reflection peaks located at 1940.52 nm and 2048.04 nm can be observed with 3 dB bandwidths of 0.15 nm and 0.17 nm, respectively. Also, for clarity, the enlarged spectra around the two reflection peaks are shown in the insets in Figure 2B.

When changing the phase mask to obtain the second Bragg wavelength, the instability of the excimer laser source and the slight vibration of the movable displacement platform led to different refractive index modulations and thus the different transmission depths. Together with the measurement error, the difference of 0.4 dB of the two transmission dips could be observed in Figure 2A. Due to the optical power of the ASE spectrum and the reflectivity of the SI-UFBG at 1940.52 nm were higher than that at 2048.04 nm, higher reflection optical power at 1940.52 nm was observed in Figure 2B, and this led to the different signal-to-noise ratio of 1940.52 nm and 2048.04 nm.

2.3 Investigation of the ASE spectrum

The ASE spectrum of the experimental configuration was investigated for different pump powers, and the experimental results are shown in Figures 3A, B. Forward and backward ASE spectra were recorded at points M and N, respectively, as shown in Figure 1. It can be seen that with an increase of pump power, the optical power of the ASE increases, and the peak wavelength shifts to the shorter-wavelength region. In addition, the optical powers at 1940.52 nm and 2048.04 nm under different pump powers when using forward and backward pumping schemes are shown in Figures 3C, D.

It can be seen in Figure 3C that when the pump power was 2.16 W, optical power at 1940.52 nm and 2048.04 nm were, respectively, ~-59.09 dB m and −59.44 dB m, and optical power difference between the two wavelengths was 0.35 dB. With an increase of pump power, optical power at 1940.52 nm increased faster than that at 2048.04 nm, and when the pump power was 3.91 W, the optical power difference between the two wavelengths reached 10.89 dB. Similarly, it can be seen in Figure 3D that when the pump power was 2.16 W, optical powers at 1940.52 nm and 2048.04 nm were, respectively, ~-51.50 dBm and −60.00 dBm, and the optical power difference between the two wavelengths was 8.49 dB. With an increase of pump power, optical power at 1940.52 nm also grew faster than that at 2048.04 nm, and when the pump power was 3.91 W, the optical power difference between the two wavelengths reached 16.21 dB. Optical power at 2048.04 nm was almost unchanged for the forward and backward pumping schemes. However, the optical power at 1940.52 nm for the backward pumping scheme was larger than that for the forward pumping scheme. Due to the optical power at 1940.52 nm for the backward pumping scheme is higher than that of the forward pumping scheme, increasing rate at 1940.52 nm for the backward pumping scheme is higher than that for forward pumping scheme. To achieve switchable output of 1940.52 nm and

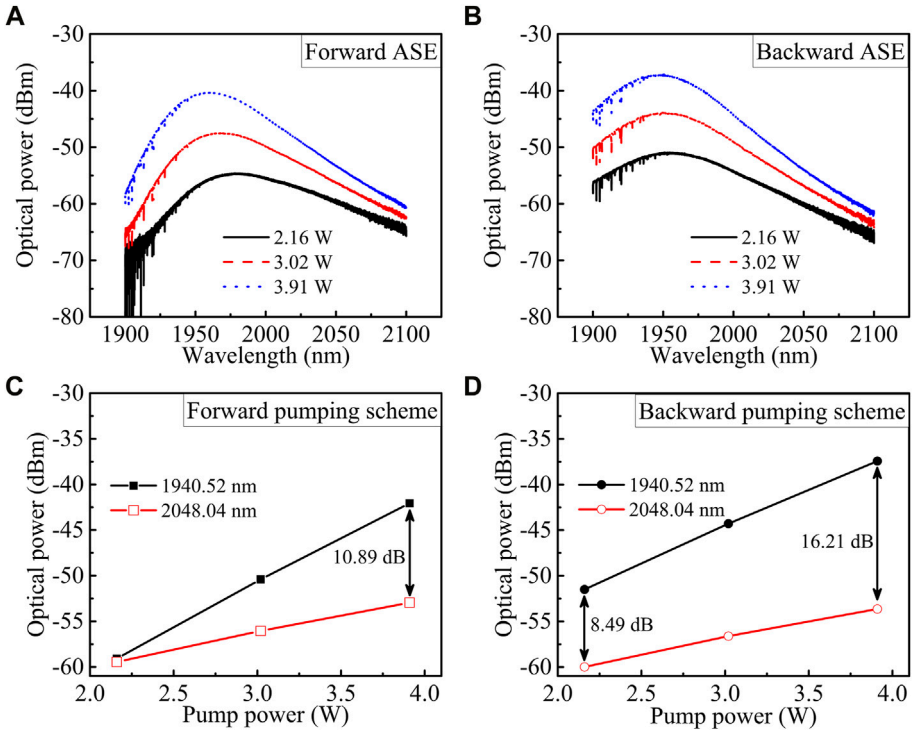

FIGURE 3
ASE spectra for different pump powers with **(A)** forward and **(B)** backward pumping scheme. Optical powers at 1940.52 and 2048.04 nm for different pump powers with **(C)** forward and **(D)** backward pumping schemes.

2048.04 nm, small optical power difference should be considered to alleviate the intense wavelength competition brought about by large optical power difference. Thus, the forward pumping scheme was selected in our experiment.

2.4 Wavelength switching mechanism

PDL was introduced by the DI-PC and in-line polarizer, and by tuning the DI-PC, wavelength switching could be achieved [38]. When the transmission light reflected by the SI-UFBG with an arbitrary polarization state passes through the DI-PC, the polarization state can be altered by rotating the DI-PC. The in-line polarizer only allows certain wavelength in a certain polarization state to pass through. Thus, through the contribution of the DI-PC and in-line polarizer, different wavelengths reflected by the SI-UFBG suffer different losses, and these are polarization dependent. Thus, PDL can be used to achieve wavelength switching [39].

3 Experimental results and discussions

3.1 Experimental results

The experiment was carried out in a laboratory at room temperature. When the pump power was fixed at 3.02 W, by tuning the DI-PC, single-wavelength output with a central wavelength of 1940.52 nm and with a high optical signal-to-noise ratio (OSNR) of ~80.90 dB could be obtained. The result, with a wavelength span of 15 nm, is shown in Figure 4A. To verify that only one lasing line was obtained, the optical spectrum with a wavelength range of 1900 nm–2,100 nm is shown in the inset of Figure 4A. A small lasing peak with optical power less than −60 dBm and an OSNR less than 10 dB could be observed, which may be attributed to the imperfect inhibition of the lasing line at 2048.02 nm, which cannot be regarded as effective lasing. Thus, single-wavelength output centered at 1940.52 nm can be achieved.

By slightly tuning the DI-PC, single-wavelength output at 2048.02 nm with a high OSNR of ~80.71 dB can be observed from the OSA. The recorded optical spectrum with a wavelength span of 15 nm is shown in Figure 4B. Also, to demonstrate that only one lasing line is output by the constructed TDFL, the output optical spectrum ranging from 1900 nm to 2,100 nm is shown in the inset of Figure 4B. Similarly, a small peak located at 1940.52 nm with an optical intensity and OSNR less than −64 dBm and 6 dB, respectively, could be observed, which also could not be regarded as effective lasing. Thus, switchable single-wavelength output between 1940.52 nm and 2048.02 nm can be achieved by tuning the DI-PC.

To verify the stability of the constructed TDFL, the output optical spectrum was recorded every 10 minutes for single-wavelength outputs with central wavelengths of 1940.52 nm and 2048.02 nm. The repeated records are shown in Figures 4C, D. When the central wavelength was 1940.52 nm, the maximum wavelength shift and optical power fluctuation were 0.04 nm and 1.09 dB, respectively, and when the

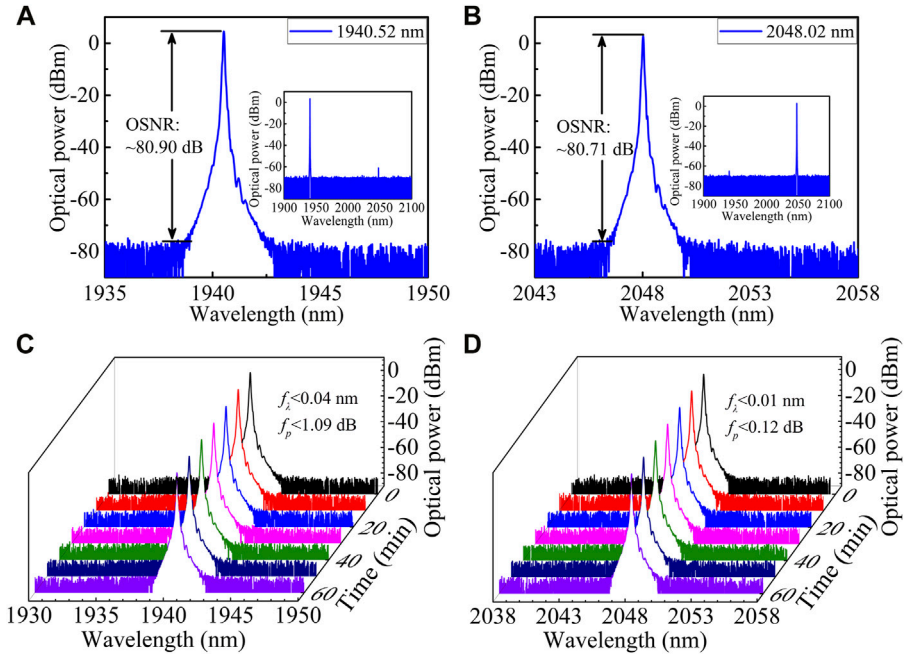

FIGURE 4
Single-wavelength output with central wavelengths of **(A)** 1940.52 nm and **(B)** 2048.02 nm. Repeated records of the optical spectrum with central wavelengths of **(C)** 1940.52 nm and **(D)** 2048.02 nm.

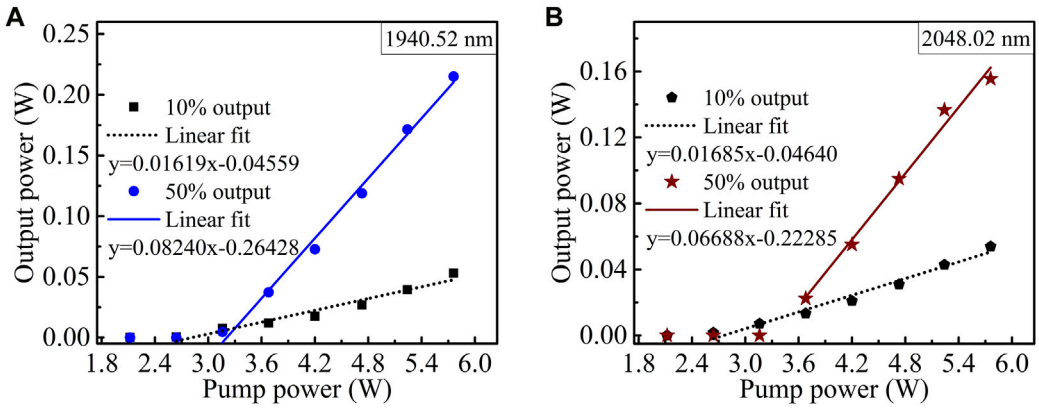

FIGURE 5
Output power versus pump power when the central wavelength is **(A)** 1940.52 and **(B)** 2048.02 nm.

lasing wavelength was 1940.52 nm, the wavelength shift and optical power fluctuation were less than 0.01 nm and 0.12 dB, respectively. These results demonstrate that the constructed TDFL can operate stably at room temperature.

The output optical power was investigated with output coupling ratios of 10% and 50% under different pump powers. Because the maximum allowable input power of the OSA was 100 mW, the output optical power was measured using a thermal sensor (A-2-D12-BBF, Laserpoint) and a power meter (Plus 2, Laserpoint). The output power for different pump powers is shown in Figure 5. Obviously, the output power increases linearly with pump power without saturation in the pump power range of 0 W–5.76 W. In the experiment, when using a high pump power, the splicing point between the output port of the FC and the input port of the TDF heated up seriously. To protect the splicing point from thermal damage, the pump power was set to 5.76 W.

When the central wavelength of the single-wavelength output was 1940.52 nm, the slope efficiencies of the TDFL were 1.62% and 8.24%, respectively, for output coupling ratio of 10% and 50%, as shown in Figure 5A. Maximum output power of 215.12 mW was obtained by using an output coupling ratio of 50% and a pump power of 5.76 W. The minimum threshold power was 2.82 W when using an output coupling ratio of 10%. Similarly, when the central wavelength of the single-

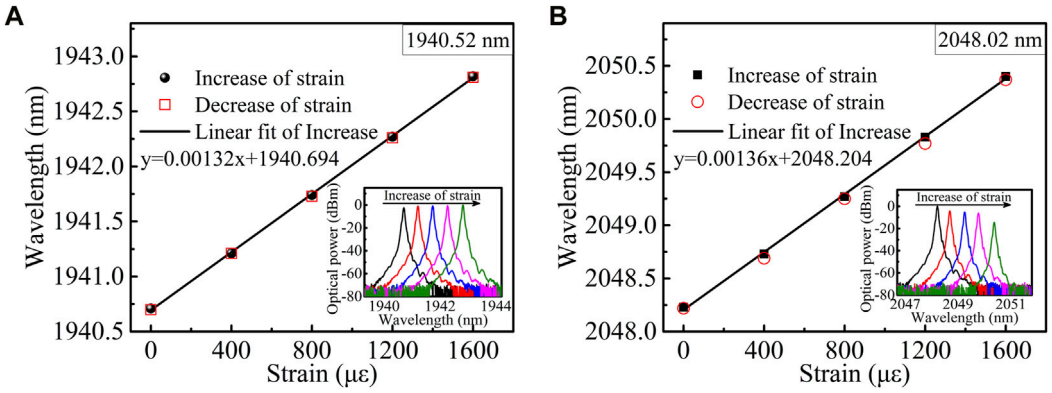

FIGURE 6
Small variations of output central wavelength as a function of strain when output wavelength is centered on **(A)** 1940.52 nm and **(B)** 2048.02 nm.

TABLE 1 Comparison of our TDFL with some of the reported wavelength switchable TDFLs based on PDL.

Maximum OSNR(dB)	Fluctuation of wavelength (nm)	Fluctuation of optical power (dB)	Operating waveband (μm)	References
~58	≤0.01	≤0.64	2.05	[23]
~55	0.02	2.78	1.94	[33]
>72	0.01	0.56	2.05	[34]
>50	0.02	0.7	1.857 to 1.927	[35]
>80	0.04	1.09	1.94 and 2.05	This work

wavelength output was 2048.02 nm, the slope efficiency of the TDFL was 1.69% for an output coupling ratio of 10%, and 6.69% for an output coupling ratio of 50%, as shown in Figure 5B. Maximum output power of 155.53 mW was obtained by using an output coupling ratio of 50% and a pump power of 5.76 W, and a minimum threshold power of 2.75 W when using an output coupling ratio of 10%.

It is to be noted that the maximal output power when the output central wavelength was 1940.52 nm was greater than that when the output central wavelength was 2048.02 nm, which is mainly attributed to the fact that the optical power at 1940.52 nm of the ASE spectrum is larger than that of the optical power at 2048.02 nm, as shown in Figure 3C. The gain obtained at 1940.52 nm was larger than that at 2048.02 nm. So, the maximum output power was obtained at 1940.52 nm.

In the experiment, two ends of the SI-UFBG were held by two fiber clamps, and the two fiber clamps were fixed at two micro-displacement stages [40]. The original distance L between the two micro-displacement stages was 25 cm, and one of the micro-displacement stages could move away from the other one with a step δl of 0.1 mm. Thus, the strain was applied to the SI-UFBG with a step of 400 με ($\delta l/L$). The change of the central wavelength with the change of applied strain can be written as:

$$\Delta\lambda = (1 - P_\varepsilon)\lambda(\delta l)/L$$

where P_ε is the effective elasto-optic coefficient, λ is the central wavelength, and (1-P_ε) is positive. Thus, with an increase of strain, the output central wavelength exhibits a "red shift."

The dependence of output central wavelength on strain is shown in Figure 6. In the experiment, the SI-UFBG used was not recoated after fabrication. According to our previous work, the strain applied on the bare SI-UFBG should not exceed 2000 με to prevent the SI-UFBG from breaking, and the maximum strain was set at 1,600 με, which restricted the tunning range of the proposed laser [25]. When the output central wavelength was 1940.52 nm, the tuning sensitivity was 0.132 pm/με, as shown in Figure 6A and a tuning range of 2.11 nm was obtained. The deviation of central wavelength was less than 0.01 nm when the applied strain increased or decreased. Variation of the output optical spectrum is also shown in the inset of Figure 6A to give a clearer presentation. When the output central wavelength was 2048.02 nm, a tuning range of 2.17 nm and a sensitivity of 0.136 pm/με were obtained, as shown in Figure 6B, where the output optical spectrum with increasing strain is shown in the inset. The output central wavelength was recorded for both increases and decreases of the applied strain, and the calculated maximum wavelength deviation was found to be 0.05 nm. These results demonstrate that the proposed TDFL is robust.

3.2 Discussions

To test the repeatability, the central wavelength was switched from 1940.52 nm to 2048.02 nm, and then switched from 2048.02 nm to 1940.52 nm. With the abovementioned process repeated five times, the deviation of central wavelength and

output power was 0.04 nm and 0.86 dB for 1940.52 nm, and 0.03 nm and 0.26 dB for 2048.02 nm.

In the experiment, by tuning the DI-PC, the laser was always operated at single-wavelength output, and dual-wavelength output was not observed. Thus, only by adjusting the DI-PC, dual-wavelength output could not be achieved under the current experimental configuration. To realize dual-wavelength output, gain competition inhibition mechanism, such as non-linear polarization rotation, should be introduced.

According to Eq. 1, the slope efficiency $(1\text{-}P_\varepsilon)\lambda$ is relate to the selected wavelength. Thus, the slope efficiency changes at different wavelengths during tuning. However, for a tuning range of 2.11 nm for 1940.52 nm, the variation of slope efficiency is ~0.109% (2.11/1940.52), which is very small and can be ignored. Similarly, for a tuning range of 2.17 nm for 2048.02 nm, the variation of the slope efficiency is ~0.106% (2.17/2048.02), which is also very small and can be ignored.

Finally, in Table 1, the proposed TDFL is compared with some of the reported TDFLs using PDL. It can be seen that the proposed TDFL in this work possesses the highest OSNR of greater than 80 dB. The fluctuation of the output central wavelength has the same order of magnitude as in reported work, and moderate optical power fluctuation was obtained. However, the proposed fiber laser could work at either 1.94 μm or 2.05 μm, which is not realized for other PDL-based wavelength switchable TDFLs.

4 Conclusion

A thulium-doped fiber laser (TDFL) was proposed and demonstrated. With the help of a drop-in polarization controller (DI-PC), in-line polarizer, and a superimposed uniform fiber Bragg grating (SI-UFBG), switchable single-wavelength outputs of 1940.52 nm and 2048.02 nm were easily achieved. For an output wavelength of 1940.52 nm, the optical signal-to-noise ratio (OSNR) was greater than 80 dB, and the fluctuations of the central wavelength and output power were, respectively, 0.04 nm and 1.09 dB, for an observation time of 60 min. Maximum output power of 215.12 mW was obtained by extracting 50% of the circulating light from the laser cavity. By applying strain on the SI-UFBG, a small tuning range of 2.11 nm was realized. For output wavelength of 2048.02 nm, the optical signal-to-noise ratio (OSNR) was 80.71 dB, and within 60 min, the fluctuations of the central wavelength and output power were, respectively, less than 0.01 nm and 0.12 dB. By using an output coupling ratio of 50%, a maximum output power of 155.53 mW was achieved. Similarly, a small tuning range of 2.17 nm was achieved. The proposed switchable TDFL may find application in biomedicine and free-space optical communication (FSOC).

Data availability statement

The raw data supporting the conclusion of this article will be made available by the authors, without undue reservation.

Author contributions

All authors listed have made a substantial, direct, and intellectual contribution to the work and approved it for publication.

Funding

This work was supported by the National Natural Science Foundation of China (Nos. 61827818, 61975105, 61975009, 61975049, and 62005013).

Acknowledgments

The authors would like to thank the editors and reviewers for their efforts in supporting the publication of this paper.

Conflict of interest

The authors declare that the research was conducted in the absence of any commercial or financial relationships that could be construed as a potential conflict of interest.

Publisher's note

References

1. Jamalus MSK, Sulaiman AH, Abdullah F, Zulkifli N, Alresheedi MT, Mahdi MA, et al. Selectable multiwavelength thulium-doped fiber laser based on parallel Lyot filter. *Opt Fiber Tech* (2022) 70:102892. doi:10.1016/j.yofte.2022.102892

2. Zhang Q, Hou Y, Song W, Wang X, Blair C, Chen X, et al. Pump RIN coupling to frequency noise of a polarization-maintaining 2 μm single frequency fiber laser. *J Opt Express* (2021) 29(3):3221–9. doi:10.1364/oe.415298

3. Li C, Shi J, Wang X, Wang B, Gong X, Song L, et al. High-energy all-fiber gain-switched thulium-doped fiber laser for volumetric photoacoustic imaging of lipids. *Photon Res* (2020) 8(2):160–4. doi:10.1364/prj.379882

4. Wittmann A, Heberle J, Huber F, Schmidt M. Consolidation of thermoplastic coatings by means of a thulium-doped fiber laser. *J Laser Appl* (2021) 33(4):042032. doi:10.2351/7.0000501

5. Wang J, Ge S, Ren H, Huang T, Yang P, Xu P, et al. High-sensitivity micro-strain sensing using a broadband wavelength-tunable thulium-doped all-fiber structured mode-locked laser. *Opt Lett* (2022) 47(1):34–7. doi:10.1364/ol.445042

6. Olson J, Ou YH, Azarm A, Kieu K. Bi-directional mode-locked thulium fiber laser as a single-cavity dual-comb source. *IEEE Photon Tech Lett* (2018) 30(20):1772–5. doi:10.1109/lpt.2018.2868940

7. Ahmad NAB, Dahlan SH, Cholan NA, Ahmad H, Tiu ZC. Switchable 10, 20, and 30 GHz region photonics-based microwave generation using thulium-doped fluoride fiber laser[J]. *JOSA B* (2018) 35(7):1603–8.

8. Żywicka B, Bujok J, Janeczek M, Czerski A, Szymonowicz M, Dobrzynski M, et al. Usefulness of thulium-doped fiber laser and diode laser in zero ischemia kidney

surgery—comparative study in pig model. *Materials* (2021) 14(8):2000. doi:10.3390/ma14082000

9. Kwiatkowski J, Sotor J. Laser wavelength shift and dual-wavelength generation in continuous-wave operation of Ho:YAG laser pumped by thulium-doped fiber laser. *Opt Laser Tech* (2022) 146:107544. doi:10.1016/j.optlastec.2021.107544

10. Chen S, Jung Y, Alam S, Richardson DJ, Sidharthan R, Ho D, et al. Ultra-short wavelength operation of thulium-doped fiber amplifiers and lasers. *Opt express* (2019) 27(25):36699–707. doi:10.1364/oe.27.036699

11. Zhang L, Zhang J, Sheng Q, Sun S, Shi C, Fu S, et al. Efficient multi-watt 1720 nm ring-cavity Tm-doped fiber laser. *Opt Express* (2020) 28(25):37910–8. doi:10.1364/oe.411671

12. Wei H, Lianqing Z, Mingli D, Fei L. A 1.8-μm multiwavelength thulium-doped fiber laser based on a hybrid interference filter. *Int J Optomechatronics* (2016) 10(3-4):154–61. doi:10.1080/15599612.2016.1230914

13. Qin Q, Yan F, Liu Y, Guo Y, Li T, Cheng D, et al. Modified two-mode fiber-based filter and its application in a switchable thulium-doped fiber laser. *Opt Laser Tech* (2022) 151:108072. doi:10.1016/j.optlastec.2022.108072

14. Fang S, Zhang Z, Yang C, Lin W, Cen X, Zhao Q, et al. Gain-switched single-frequency DBR pulsed fiber laser at 2.0 μm. *IEEE Photon Tech Lett* (2022) 34(5):255–8. doi:10.1109/lpt.2022.3149525

15. Guo Y, Yan F, Feng T, Qin Q, Cheng D, Guan B, et al. Multi-wavelength thulium-doped fiber laser at 2.05 μm incorporating a superimposed polarization-maintaining fiber Bragg grating. *Infrared Phys Tech* (2022) 122:104046. doi:10.1016/j.infrared.2022.104046

16. Żywicka B, Rybak Z, Janeczek M, Czerski A, Bujok J, Szymonowicz M, et al. Comparison of A 1940 nm thulium-doped fiber laser and A 1470 nm Diode laser for cutting efficacy and hemostasis in A pig model of spleen surgery. *J Mater* (2020) 13(5):1167. doi:10.3390/ma13051167

17. Tendean M. Role of thulium doped fiber laser (TDFL) 1940 nm in liver resection for secondary liver tumors, a single center experience. *HPB* (2022) 24:S604–5. doi:10.1016/j.hpb.2022.05.1318

18. McComb TS, Shah L, Sims RA, Willis CCC, Kadwani P, Sudesn V, et al. Atmospheric propagation testing with a high power, tunable thulium fiber laser system[C]//Solid State Lasers XIX: Technology and Devices. *SPIE* (2010) 7578:362–8.

19. Guan B, Yan F, Feng T, Han W, Qin Q, Zhang L, et al. Preliminary demonstration of text and real-time video transmission in free space optical communication system at 2 μm band[C]//Eighth Symposium on Novel Photoelectronic Detection Technology and Applications. *SPIE* (2022) 12169:2334–9.

20. Cheng D, Yan F, Feng T, Han W, Zhang L, Qin Q, et al. Five-wavelength-switchable single-longitudinal-mode thulium-doped fiber laser based on a passive cascaded triple-ring cavity filter. *IEEE Photon J* (2021) 14(1):1–8. doi:10.1109/jphot.2021.3128165

21. Latiff AA, Shamsudin H, Ahmad H, Harun S. Q-switched thulium-doped fiber laser operating at 1940 nm region using a pencil-core as saturable absorber. *J Mod Opt* (2016) 63(8):783–7. doi:10.1080/09500340.2015.1100342

22. Zhang L, Sheng Q, Chen L, Zhang J, Fu S, Fang Q, et al. Single-frequency Tm-doped fiber laser with 215 mW at 2.05 μm based on a Tm/Ho-codoped fiber saturable absorber. *Opt Lett* (2022) 47(15):3964–7. doi:10.1364/ol.463202

23. Guo Y, Yan F, Feng T, Qin Q, Han W, Cheng D, et al. Wavelength-switchable single-longitudinal-mode thulium-doped fiber laser at 2.05 μm using a superimposed fiber Bragg grating. *Infrared Phys Tech* (2022) 122:104058. doi:10.1016/j.infrared.2022.104058

24. Walasik W, Traoré D, Amavigan A, Tench RE, Delavaux JM, Pinsard E. 2-μm narrow linewidth all-fiber DFB fiber Bragg grating lasers for Ho- and Tm-doped fiber-amplifier applications. *J Lightwave Tech* (2021) 39(15):5096–102. doi:10.1109/jlt.2021.3079235

25. Qin Q, Yan F, Liu Y, Cheng D, Yu C, Yang D, et al. Thulium-doped fiber laser with bidirectional output in a ring laser cavity. *Opt Laser Tech* (2022) 155:108390. doi:10.1016/j.optlastec.2022.108390

26. Escobar EH, Jiménez MB, Avilés AC, Lopez Estopier R, Pottiez O, Duran Sanchez M, et al. Experimental study of an in-fiber acousto-optic tunable bandpass filter for single- and dual-wavelength operation in a thulium-doped fiber laser. *Opt express* (2019) 27(26):38602–13. doi:10.1364/oe.382166

27. Chen X, Dai D, Zhang Y, Wu H, Gao Y, Chen G, et al. Wavelength-flexible thulium-doped fiber laser based on digital micromirror array. *Micromachines* (2020) 11(12):1036. doi:10.3390/mi11121036

28. Liu F, Liu P, Feng X, Wang C, Yan Z, Zhang Z. Tandem-pumped, tunable thulium-doped fiber laser in 21 μm wavelength region. *Opt express* (2019) 27(6):8283–90. doi:10.1364/oe.27.008283

29. Guo Y, Yan F, Feng T, Qin Q, Zhang L, Guan B, et al. Stable multi-wavelength thulium-doped fiber laser with two cascaded single-mode-four-mode-single-mode fiber interferometers[J]. *IEEE Access* (2020) 9:1197–204.

30. Posada-Ramírez B, Durán-Sánchez M, Álvarez-Tamayo RI, Ibarra-Escamilla B, Bravo-Huerta E, Kuzin EA. Study of a Hi-Bi FOLM for tunable and dual-wavelength operation of a thulium-doped fiber laser. *Opt express* (2017) 25(3):2560–8. doi:10.1364/oe.25.002560

31. Ibarra-Escamilla B, Durán-Sánchez M, Álvarez-Tamayo RI, Posada-Ramirez B, Prieto-Cortes P, Kuzin EA, et al. Tunable dual-wavelength operation of an all-fiber thulium-doped fiber laser based on tunable fiber Bragg gratings. *J Opt* (2018) 20(8):085702. doi:10.1088/2040-8986/aad25b

32. Qin Q, Yan F, Liu Y, Cui Z, Dan C, Yu C, et al. Twelve-wavelength-switchable thulium-doped fiber laser with a multimode fiber Bragg grating. *IEEE Photon J* (2021) 13(3):1–10. doi:10.1109/jphot.2021.3084929

33. Guo Y, Yan F, Feng T, Zhang L, Qin Q, Han W, et al. Switchable multi-wavelength thulium-doped fiber laser using four-mode fiber based sagnac loop filter. *IEEE Photon J* (2020) 12(2):1–10. doi:10.1109/jphot.2020.2973671

34. Cheng D, Yan F, Feng T, Zhang L, Han W, Qin Q, et al. Six-wavelength-switchable SLM thulium-doped fiber laser enabled by sampled FBGs and 3 × 3 coupler based dual-ring compound cavity filter. *IEEE Photon J* (2022) 14(2):1–8. doi:10.1109/jphot.2022.3147223

35. Jia C, Liang X, Rochette M, Chen LR. Alternate Wavelength Switching in a Widely Tunable Dual-Wavelength Tm <named-content content-type=math xlink:type=simple> <inline-formula> <tex-math notation=TeX>${3+}$</tex-math></inline-formula></named-content>-Doped Fiber Laser at 1900 nm. *IEEE Photon J* (2015) 7(4):1–7. doi:10.1109/jphot.2015.2451654

36. Feng T, Jiang M, Wei D, Zhang L, Yan F, Wu S, et al. Four-wavelength-switchable SLM fiber laser with sub-kHz linewidth using superimposed high-birefringence FBG and dual-coupler ring based compound-cavity filter. *Opt express* (2019) 27(25):36662–79. doi:10.1364/oe.27.036662

37. Feng T, Su J, Wei D, Li D, Li C, Yan F, et al. Effective linewidth compression of a single-longitudinal-mode fiber laser with randomly distributed high scattering centers in the fiber induced by femtosecond laser pulses. *Opt Express* (2023) 31(3):4238–52. doi:10.1364/oe.482083

38. Li Y, Shen Y, Tian J, Fu Q, Yao Y. Wavelength switchable multi-wavelength erbium-doped fiber laser based on polarization-dependent loss modulation. *J Lightwave Tech* (2021) 39(1):243–50. doi:10.1109/jlt.2020.3026693

39. Feng T, Ding D, Yan F, Zhao Z, Su H, Yao XS. Widely tunable single-/dual-wavelength fiber lasers with ultra-narrow linewidth and high OSNR using high quality passive subring cavity and novel tuning method. *Opt Express* (2016) 24(17):19760–8. doi:10.1364/oe.24.019760

40. Feng T, Wei D, Bi W, Sun W, Wu S, Jiang M, et al. Wavelength-switchable ultra-narrow linewidth fiber laser enabled by a figure-8 compound-ring-cavity filter and a polarization-managed four-channel filter. *Opt Express* (2021) 29(20):31179–200. doi:10.1364/oe.439732